



## ORIGINAL ARTICLE

# Characterization of plants and seaweeds based corrosion inhibitors against microbially influenced corrosion in a cooling tower water environment



Mohamad S AlSalhi<sup>a,\*\*</sup>, Sandhanasamy Devanesan<sup>a</sup>, Aruliah Rajasekar<sup>b</sup>,  
Seenivasan Kokilaramani<sup>b,\*</sup>

<sup>a</sup> Department of Physics and Astronomy, College of Science, King Saud University, P. O. Box 2455, Riyadh 11451, Saudi Arabia

<sup>b</sup> Environmental Molecular Microbiology Research Laboratory, Department of Biotechnology, Thiruvalluvar University, Serkkadu, Vellore, Tamilnadu 632115, India

Received 1 August 2022; accepted 6 December 2022

Available online 12 December 2022

## KEYWORDS

Green Inhibitors;  
*Pseudomonas stutzeri*;  
Mild Steel;  
Cooling Tower Water;  
Microbial Influenced  
Corrosion

**Abstract** This study compares the inhibitory activities of methanolic extraction of various plants including *Artemisia pallens* (MEAP), mangrove leaves like *Rhizophora mangle* (MERM), *Avicennia marina* (MEAM) and seaweeds such as *Pandia povanica* (MEPP), *Sargassum tenerrimum* (MEST) on the corrosion of mild steel (MS) coupons that were incubated on *Pseudomonas stutzeri* (*P. stutzeri*) SKR4 strain isolated from the cooling tower water (CTW). The activities of inhibitors are found using GCMS analysis and interactions between microbes and inhibitors were examined in the test for antibacterial activity, minimal inhibition concentration, biofilm formation assay. These all show an excellent inhibitory effect against *P. stutzeri*. The weight loss, impedance spectroscopy, and Tafel polarization tests used to validate the corrosion investigations show that the inhibitors MEAP-75, MERM-71, MEAM-69, MEPP-66 and MEST-63 % are effective at inhibiting corrosion at 25 ppm. According to Potentiodynamic polarization plots, these five inhibitors act as mixed-type inhibitors. The surface investigation of MS metals by FTIR, SEM, XRD to examine the biofilm surface and it revealed deep pitting corrosion in the bacterial system. In the conclusion, eco-friendly green inhibitors have controlled the biocorrosion in cooling tower water and are recommended for usage in industries as an alternative to environmentally hazardous inhibitors.

© 2022 The Authors. Published by Elsevier B.V. on behalf of King Saud University. This is an open access article under the CC BY-NC-ND license (<http://creativecommons.org/licenses/by-nc-nd/4.0/>).

\* Corresponding author.

E-mail addresses: [malsalhi@ksu.edu.sa](mailto:malsalhi@ksu.edu.sa) (M.S AlSalhi), [ramaniseenivasan@gmail.com](mailto:ramaniseenivasan@gmail.com) (S. Kokilaramani).

Peer review under responsibility of King Saud University.



## 1. Introduction

Corrosion is one of the most severe threats in today's industrial and marine environment because it can swiftly degrade metals through oxidation and reduction of chemical and electrochemical processes (Ismail et al., 2022; Quraishi et al., 2021). Microbially influenced corrosion (MIC) is a kind of corrosion induced by extracellular polymeric substances secreted by microorganisms like bacteria (Rossell6-Moral9 et al., 1994), fungi (Obot et al., 2009; Rajasekar et al., 2010), archaea, and algae (Ismail et al., 2022), which creates a biofilm layer on the metal surface and causes the metals distraction (Kakooei et al., 2012; Zhang et al., 2022). An unbalanced physio and electrochemical process in the electrolytes such as pH, metal composition, temperature, and electrolyte interactions resulted in a large production of microorganisms. Biofilm layers are formed when microorganisms produce extra polymeric substances (EPS) like proteins, carbohydrates, and lipids, which leads to increased microbial adhesion and corrosion of metals properties (Oguzie et al., 2005). The MIC causes inflict severe economic losses throughout the world; the IMPACT (International Measures of Prevention, Application, and Economics of Corrosion Technology) studies estimate that the worldwide corrosion cost is 3–4 % of gross domestic product (GDP) annually (Zehra et al., 2022). The National Association of Corrosion Engineers (NACE) reported corrosion costs the oil and gas industries more than US\$60 billion per annum.

In the industrial sectors, the equipments are released a significant amount of heat because of the outcomes of the operating process. During working hours, it's important to keep the equipment's temperature stable and eliminate heat (Narenkumar et al., 2021). Cooling towers are employed in all of that as the standard and necessary equipment to maintain the temperature in all industrial processing equipment. It is extremely sensitive to corrosion due to the ideal environment, which includes a constant flow of liquids with dissolved salts, temperature, pH, and microbial growth (biofilm formation) (Ahmed and Makki, 2019).

Corrosion is a chemical and electrochemical process through a reduction and oxidation reaction of potential in different sites on the metal surface. Generally, mild steel (MS) is widely utilized in industries to build cooling tower systems due to its low carbon steel, long-lasting and affordable. It is prone to corrosion due to the cooling tower's lack of maintenance conditions and its thermodynamic stability (Popova et al., 2018; Wagner et al., 2018). The corrosion process in cooling tower systems significantly hampered the breakdown of thermal stability, structural damage, and water flows interpretation, finally forcing a shutdown of the entire system (Kuraimid et al., 2021). Mostly cooling towers creates pitting types of corrosion due to the biofilm formation by microbial adhesion on metals surface (Suharso et al., 2017). For metal protection from corrosion activities, the inhibitors are used to prevent metal distraction through the formation of protective barriers against microbial interaction or to limit the growth of biofilm from destructive assaults of microbes (Popova et al., n.d.). According to a scientific report, economic losses from corrosion are minimized by up to 15 % (US \$375 billion) to 35 % (US \$875 billion) by using inhibitors (Verma et al., 2021). One of the most popular methods of preventing corrosion is the use of inhibitors, these organic or inorganic compounds can slow down the rate of corrosion and are normally added in very small quantities to the corrosive medium to prevent metal corrosion (Cherrad et al., 2022).

Organic inhibitors are commonly employed in the inhibition process based on the fact they are environmentally safe, renewable, non-hazardous and have a minimal toxic effect (Maleki et al., 2016). The organic molecules with heteroatoms like oxygen, nitrogen, sulphur act as the most effective inhibitors of microbial corrosion in industrial processes (Ahmed and Makki, 2019). The plant and marine extracts are natural compounds of amino acids, polysaccharides, flavonoids and other compounds of highly unshared electron pairs to create coordination bonds with the vacant orbitals, non-bonded lone pair, and  $\pi$

electrons that prevent metal corrosion by adsorption and electron donation to the metal that allows them to remove adsorbed water molecules from the metallic surface (Cherrad et al., 2022; K. M. O. Goni and A. J. Mazumder, 2019; Wang et al., 2022; Zakeri et al., 2022).

This study aims to investigate the effects of green corrosion inhibitors like plant leaf (*Artemisia pallens*), mangrove leaves (*Rhizophora mangle*, *Avicennia marina*) and seaweeds (*Pandia povanica*, *Sargassum tenerrimum*) on the MS of corrosive bacterium (*P. stutzeri*). The inhibitors were evaluated by various biological studies (bacterial activity, minimal inhibitory concentration and biofilm assay). The weight loss, EIS, potentiodynamic polarization, GC–MS, FT-IR, SEM, and XRD analysis were used to understand microbially induced corrosion/corrosion inhibition processes.

## 2. Materials and method

### 2.1. Test organism

The corrosive bacterium of *Pseudomonas stutzeri* ( $2.2 \times 10^6$  (approximately  $10^6$  colony-forming unit/milliliter (CFU/mL))) was used in the experimental part of this study, and it was isolated from the cooling tower water collected from Ranipet Tannery Effluent Treatment Ltd., Ranipet, Tamilndau. The isolated strain was cultured on the Luria-Bertani (LB) medium with the optimum condition (Kokilaramani et al., 2020).

### 2.2. Biochemical analysis

The identified bacterial culture was inoculated in the selective media of MacConkey agar and incubated for 16 h at 37 °C. After incubation, the isolated single colony was tested for biochemical tests (Kamil and Al-Hassani, n.d.).

### 2.3. Inhibitors preparation

The methanolic extraction of green inhibitors was extracted from various samples of plant leaf *Artemisia pallens* (MEAP) (Kokilaramani et al., 2020), *Rhizophora mangle* (MERM), *Avicennia marina* (MEAM) (Kokilaramani et al., 2022), and seaweeds *Pandia povanica* (MEPP), *Sargassum tenerrimum* (MEST) (Kokilaramani et al., 2021b). The green inhibitors were extracted by using the Soxhlet extraction method under optimal conditions. Following the extraction, it was filtered with a syringe filter (0.2  $\mu$ m) before being dried in oven. The dried material was stored in the refrigerator for further examination (Zaher et al., 2022).

### 2.4. Gas chromatography-mass spectrometry (GC–MS) analysis

The inhibitor components were analysed by Agilent 7890A (GC) and 5975C (Mass Spectrometer) instrument, 1  $\mu$ L of MEAP, MERM, MEAM, MEPP and MEST loaded in the column HP5-MS, injector volume of 1  $\mu$ L of carrier gas (helium) with a 1.0 mL/min of flow rate. and the oven was pre-heated to 55 °C for 2 mins, increased to 70 °C/min, detector temperature of 225 °C, the overall running time is 35.5 mins and the compounds are identified by comparing the findings to the matching mass spectra in the library data (NIST05.LIB) (al Otaibi and Hammud, 2021; Mobin et al., 2020).

### 2.5. Antibacterial activity

The antibacterial activity of MEAP, MERM, MEAM, MEPP and MEST against SKR4 was determined using the agar diffusion technique. The bacterial strain was swapped on Muller Hinton Agar (MHA) plates and the agar was diffused with a gel puncher before adding the inhibitors, positive control (Ampicillin), and negative control (Double Distilled Water (D.D H<sub>2</sub>O)). The plates were incubated at 37 °C for 24 h and to assess the antibacterial activity of inhibitors, a diameter of the bacterial inhibition zone in millimeters (mm) was determined (Oduote and Ajayi, 2013).

### 2.6. Minimal inhibition concentration assay

MIC assay was carried out in the broth dilution method on the different concentrations (10, 25, 50, 75 and 100 ppm) of green inhibitors (MEAP, MERM, MEAM, MEPP, MEST) were taken against the SKR4 bacterial strain in Mueller Hinton Broth (MHB). After the inhibition period, samples were examined in optical density (OD) values for each sample, the experiment was done in a triplet (Thakur and Kumar, 2021).

### 2.7. Enumeration of total viable count (TVC)

The bacterial count was performed by the serial dilution of incubators (MEAP, MERM, MEAM, MEPP, MEST) in different concentrations (10, 25, 50, and 100 ppm) on the MH Agar plates in spread plate method and the colony counts were done after the period of incubation for 24 h at 37 °C, it was denoted as CFU/mL (Feijoo-Siota et al., 2008).

### 2.8. Biofilm inhibition assay

The impact of green inhibitors at various concentrations on SKR4 for biofilm inhibition was assessed using a crystal violet (CV) test as earlier described (Pipattanachat et al., 2021). The log-phase bacterial culture SKR4 was resuspended in the MH broth and added to 96 well microtiter plate by following systems. A Total number of biofilm formation systems is 12 (n = 12) were placed on the 96-well microtitre plate with 1 mL of MHB (control) standard for all methods. System 1 (S1) - Control; System 2 (S2) - S1 + 100 µL of (0.500 OD) SKR4 culture; System 3 (S3) - S2 + 25 ppm of MEAP; System 4 (S4) - S1 + 25 ppm of MEAP; System 5 (S5) - S2 + 25 ppm of MERM; System 6 (S6) - S1 + 25 ppm of MERM; System 7 (S7) - S2 + 25 ppm of MEAM, System 8 (S8) - S1 + 25 ppm of MEAM, System 9 (S9) - S2 + 25 ppm of MEPP, System 10 (S10) - S1 + 25 ppm of MEPP, System 11 (S11) - S2 + 25 ppm of MEST, System 12 (S12) - S1 + 25 ppm of MEST. The plate was incubated for 24 h at 37 °C to induce biofilm growth. After incubation, wash the area with phosphate-buffered saline (PBS, pH-7.4) to remove any adhering microorganisms. The biofilms were treated for 20 mins at room temperature (RT) in 70 % ethanol and it was withdrawn from each well then 200 µL of 1 % crystal violet dye was added for staining in 20 mins. It was washed three times in PBS to get rid of the remaining color and each well received 500 µL of 30 % acetic acid to elute the excess dye. After 10 mins of incubation, the results were assessed at 570 nm using a UV-Visible

spectrophotometer and the system of biofilm assay was done in triplicate (Karunakaran and Biggs, 2011).

### 2.9. Specimen preparation

The Mild Steel 1010 (MS 1010) coupons employed with a percent composition of Si- 0.002, S-0.026, P-0.01, Ni-0.04, Mo-0.002, Mn-0.16, Fe-99.64, Cu-0.093, C-0.03. For weight loss, it was cut into 2.5 cm<sup>2</sup> by 2.5 cm<sup>2</sup> with a 2 mm hole, SEM examination, 1 cm<sup>2</sup> by 1 cm<sup>2</sup> with a 1 mm hole at the top for hanging reasons and 1 cm<sup>2</sup> by 1 cm<sup>2</sup> for electrochemical study (working electrode (WE)). The surface of the specimen was polished with different grade sheets and cleaned in trichloroethylene, rinsed on D.D H<sub>2</sub>O and sterilized with acetone and ethanol, before being kept in the desiccator, specimens were air-dried. The experimental coupons were treated under UV light exposure for 30 mins before starting the experiments (Kokilaramani et al., 2021b).

### 2.10. Weight loss (WL) method

A weighted sample (coupon – 2.5 cm<sup>2</sup> × 2.5 cm<sup>2</sup>) of the MS 1010 was introduced into the SKR4 and different inhibitors. A Total number of biofilm formation systems is 12 (n = 12) were placed on a 500 mL conical flask with 400 mL of autoclaved CTW with 1 % NB medium (control) common for all methods. System 1 (S1) - Control; System 2 (S2) - S1 + 100 µL of (0.500 OD) SKR4 culture; System 3 (S3) - S2 + 25 ppm of MEAP; System 4 (S4) - S1 + 25 ppm of MEAP; System 5 (S5) - S2 + 25 ppm of MERM; System 6 (S6) - S1 + 25 ppm of MERM; System 7 (S7) - S2 + 25 ppm of MEAM, System 8 (S8) - S1 + 25 ppm of MEAM, System 9 (S9) - S2 + 25 ppm of MEPP, System 10 (S10) - S1 + 25 ppm of MEPP, System 11 (S11) - S2 + 25 ppm of MEST, System 12 (S12) - S1 + 25 ppm of MEST in triplicate with the immobile condition. The specimen was taken out of the flask after 21 days of exposure, then non-metallic scrapers were used to remove the biofilm layers. It was reweighed after being cleaned with a pickling solution (Narenkumar et al., 2017a) to get rid of all corrosion products. According to ASTM G1, the MS corrosion rate was assessed and reported in mils per year (mpy) and the weight loss calculation is converted as a Corrosion Rate (CR) as followed

$$CR = \frac{\text{Weight loss (g)} * \text{Constant (K)}}{\text{Density of Alloy (g/cm}^3\text{)} * \text{Exposed Area (A)} * \text{Exposure Time (h)}} \quad (1)$$

The following formulae were used to obtain the % Inhibition Efficiency (IE):

$$\%IE = \frac{W-W1}{W} \times 100 \text{ where } W \text{ and } W1 \text{ stand for metal weight loss without and with inhibitors, respectively.}$$

### 2.11. Fourier transform infrared spectrophotometers (FT-IR) analysis

The biofilm-formed coupons (12 samples) were adequately dried after the WL study. The dried samples were blended on KBr to make the shape into a pellet. The pellets were subjected to using FT-IR spectra with a range of 400–4000 cm<sup>-1</sup> wave number, 8 cm<sup>-1</sup> resolution and 64 scans/spectrum scan

rate spectra (PerkinElmer Spectrum IR Version 10.6.0) (Rajasekar et al., 2008).

### 2.12. Scanning electron microscopy (SEM) analysis

SEM analysis was carried out Tescan VEGA 3SBH model make with high magnification and resolution. The MS samples were done for both with or without inhibitors and bacteria in a corrosive solution. After 21 days of exposure, the specimen surfaces S1, S2, S3, S5, S7, S9, S11 were examined in order to assess the surface microstructure and composition of biofilm formation (Huang et al., 2022).

### 2.13. X-ray diffraction (XRD) studies

The S1, S2, S3, S5, S7, S9, S11 systems scaped metallic dry powdered samples were analyzed by XRD on a Bruker D8 Advance made with a LynxEye & Scintillation Counter detector of 5° to 140° angular range and the power is 40KV;30KV (Muthukrishnan et al., 2017).

### 2.14. Electrochemical method

Electrochemical tests were performed on coupons with a diameter of 1 cm<sup>2</sup> were implanted in a specimen holder. A working electrode as MS 1010 coupon, a counter electrode a platinum mesh with low impedance, and a reference electrode as a saturated calomel electrode (SCE) was used on the system (12 systems). The Version of Nova 2.1.5 Metrohm Autolab electrochemical system was used to analyze the behavior at 30 ± 1 °C and each value of the studies is conducted in triplicate (Kokilaramani et al., 2021b).

## 3. Results

### 3.1. Biochemical analysis

The fresh colonies on MacConkey agar plate, isolates were identified initially by their typical wrinkled, unusual shape, adherent, non-pigment, dry, light yellow color colony morphology. The Gram staining and biochemical test results shown in Table 1 were analyzed for specific bacterial confirmation. The results of gram staining are Gram-negative, rod-like structure, motile, and single polar-flagellated organism (Rossell6-Moral9 et al., 1994). Biochemical tests revealed that the strain is a *P. stutzeri* species: oxidase, catalase-positive bacteria, citrate utilization, nitrate reduction and gelation hydrolysis. It is an aerobic, nonfermenting, active, nonfluorescent denitrifying bacteria with respiratory metabolic activities using oxygen as the terminal electron receptor (Lalucat et al., 2006).

### 3.2. Bacterial identification

The corrosive bacterium of *Pseudomonas stutzeri* SKR4 was isolated from the CTW sample and it was confirmed by 16S rRNA sequencing and phylogenetic tree shows Fig. 1 that 99 % of sequences are similar to the *P. stutzeri* and it was submitted to NCBI GenBank the accession number as MT211552.1 (Kokilaramani et al., 2020).

**Table 1** Biochemical Analysis of *P. stutzeri* SKR4.

Biochemical Test	Results
Gram stain	–
Shape	Rod
Motility	Motile
Catalase	+
Oxidase	+
Methyl red	+
Hydrogen sulfide production	–
Indole	–
Voges-Proskauer	–
Oxidative/Fermentative	Oxidative
Lactose	–
Citrate utilization	+
Sucrose utilization	–
Nitrate reduction	+
Gas	+
Lysine decarboxylase	–
Ornithine decarboxylase	–
Arginine decarboxylase	–
Urea hydrolysis	–
Esculin hydrolysis	–
Starch hydrolysis	–
Gelatin hydrolysis	+

(– Negative; + Positive)

### 3.3. Gas chromatography-mass spectrometry (GC–MS) analysis

The GC–MS analysis of green inhibitors MEAP, MERM, MEAM, MEPP and MEST have identified compounds provided in Table 2 Fig. 2. The GC–MS study showed a wide range of compounds are found as *n*-Hexadecanoic acid, Myo-inositol, 4-C-methyl and Lupeol, trifluoroacetate Hep-tasiloxane, 1,1,3,3,5,5,7,7,9,9,11,11,13,13- tetradecamethyl-substances to control the microbial activity. The obtained inhibitor substances prevent biofilm formation and control the corrosion process in the CTW (Khattab et al., 2012).

### 3.4. Antibacterial activity against *P. Stutzeri*

The results of antibacterial activity in the green inhibitors diameter of the inhibition zone (mm) were shown in Table 3, while 26 mm MEAP has a robust bacteriostatic impact, the rest of the inhibitors: 19 mm MERM, 15 mm MEAM, 11 mm MEPP and 8 mm MEST also show a decent zone of inhibition against SKR4 bacterial strain. As predicted, the sterile DDH<sub>2</sub>O negative control was inactive against tested bacteria and the positive control Ampicillin as a clear zone is observed. All these five inhibitors show effective antibacterial properties, non-hazardous, easy to use and have no side effects. Therefore, they might be utilized as microbial corrosion inhibitors (Narenkumar et al., 2018; Obot et al., 2009).

### 3.5. Minimal inhibition concentration assay

MIC of SKR4 against the five green inhibitors of MEAP, MERM, MEAM, MEPP, MEST at different concentrations (10, 25, 50, 75 and 100 ppm) was evaluated and shown in Table 3, the OD values (µg/mL) of the inhibitors at 25 ppm

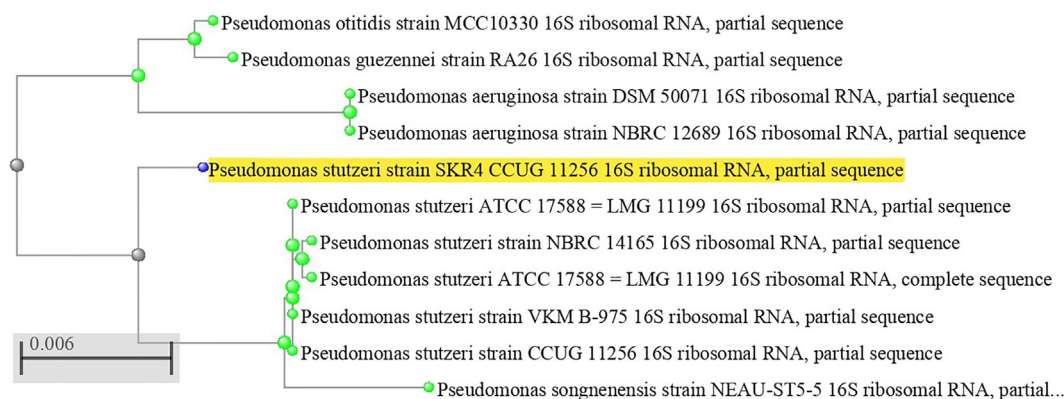


**Fig. 1** Neighbor Joining Phenogram Shows Phylogenetic Position of Strain SKR4 within the Genus *Pseudomonas* Based on 16S rRNA Gene Sequence Analysis.

**Table 2** GCMS Analysis of Green Inhibitors.

Component RT	Compound Name	Formula	Area %
<b>MEAP</b>			
19.6736	<i>n</i> -Hexadecanoic acid	C16H32O2	34.92
22.4400	Pallensin	C15H20O4	11.54
3.9070	Cyclohexane, ethyl-	C8H16	8.001
22.0530	1,14-Tetradecanediol	C14H30O2	7.209
3.1620	Cyclohexane, 1,3-dimethyl-, trans-	C8H16	6.646
3.2775	Cyclopentane, 1-ethyl-1-methyl-	C8H16	6.106
22.5670	1-Iododec-1-yne	C10H17I	5.856
3.5085	Cyclohexane, 1,3-dimethyl-, trans-	C8H16	5.388
15.1804	Hexane, 3-methoxy-	C7H16O	4.523
3.4103	2-Heptanol, 5-methyl-	C8H18O	2.568
<b>MERM</b>			
16.6588	Myo-Inositol, 4-C-methyl-	C7H14O6	94.36
17.2825	5,5,8a-Trimethyl-3,5,6,7,8,8a-hexahydro-2Hchromene	C12H20O	0.6992
19.6735	Nonanoic acid	C9H18O2	0.5262
3.9069	Cyclohexane, ethyl-	C8H16	0.524
22.2493	Pyrene	C16H10	0.44
3.1619	Cyclohexane, 1,2-dimethyl-, trans-	C8H16	0.3747
19.8468	3-Phenanthrol	C14H10O	0.2713
17.3923	9H-Fluorene, 9-methylene-	C14H10	0.2332
3.4102	Cyclopentane, 1,1,2-trimethyl-	C8H16	0.1694
18.8823	1,1'-Bicyclohexyl, 2-propyl-, trans-	C15H28	0.1677
<b>MEAM</b>			
32.2465	Lupeol, trifluoroacetate	C32H49F3O2	65.35
30.9066	.beta.-Amyrin	C30H50O	11.51
16.0583	Hexane, 3-methoxy-	C7H16O	3.325
3.1621	Cyclohexane, 1,4-dimethyl-	C8H16	3.193
<b>MEPP</b>			
16.5434	Myo-Inositol, 4-C-methyl-	C7H14O6	92.99
17.2769	5,5,8a-Trimethyl-3,5,6,7,8,8a-hexahydro-2Hchromene	C12H20O	0.5916
3.1621	Cyclohexane, 1,3-dimethyl-, trans-	C8H16	0.4994
15.2151	Butane, 2-methoxy-2-methyl-	C6H14O	0.3622
17.8775	3-Ethyl-4-methyl-3-heptanol	C10H22O	0.2451
19.0788	Decanoic acid, 2-methyl-	C11H22O2	0.1171
<b>MEST</b>			
32.2465	Heptasiloxane, 1,1,3,3,5,5,7,7,9,9,11,11,13,13-tetradecamethyl-	C14H44O6Si7	90.86
19.6794	<i>n</i> -Hexadecanoic acid	C16H32O2	1.665
3.1621	Cyclohexane, 1,3-dimethyl-, trans-	C8H16	1.464
16.7282	6-Hydroxy-4,4,7a-trimethyl-5,6,7-tetrahydrobenzofuran-2(4H)-one	C11H16O3	0.9348
3.4046	2-Heptanol, 5-methyl-	C8H18O	0.5464
17.8775	Ethanol, 2-(2-propenyloxy)-	C5H10O2	0.3546
22.4573	Cyclohexane, 1-isopropyl-1-methyl-	C10H20	0.3306

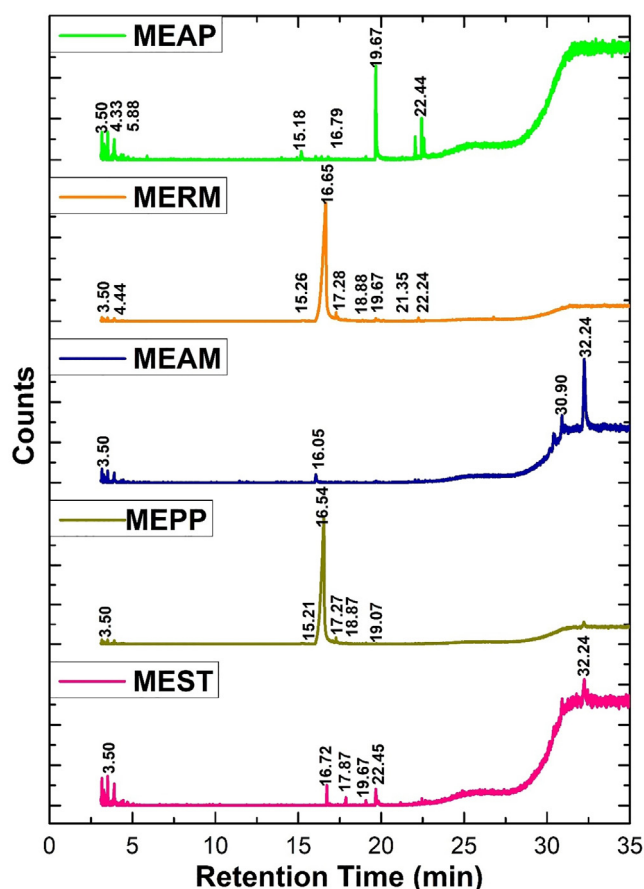


**Fig. 2** GCMS Analysis for Methanolic Extraction of Green Inhibitors.

of concentration manifested as a high bacterial resistance than other concentrations and MEAP  $18.18 \pm 1$  is more efficient compared to others. As for the other inhibitors MERM  $26.47 \pm 1$ , MEAM  $29.25 \pm 1$ , MEPP  $42.51 \pm 1$ , MEST  $45.13 \pm 1$ . Green inhibitors are the ability to act against microbial activities and control their growth (Okeniyi et al., 2019).

### 3.6. Enumeration of total viable count (TVC)

The impact of different concentrations (10, 25, 50, 75 and 100 ppm) of inhibitors on an SKR4 strain was evaluated (CFU/mL) and shown in Table 3. The results of this study showed that 25 ppm of the concentration has MEAP  $1.0 \times 10^2$ , MERM  $2.5 \times 10^3$ , MEAM  $1.8 \times 10^3$ , MEPP  $2.5 \times 10^3$ , MEST  $3.1 \times 10^3$ , gradually decreased colony formation on the plates when compared to other concentrations, and

in that MEAP has higher inhibition efficiency (Kokilaramani et al., 2021b).

### 3.7. Biofilm inhibition assay

The crystal violet method was employed in the biofilm assay against SKR4. The results of 96 well microtiter plate wide range of color variations that are visible to the naked eye (Wang et al., 2017). The control S1, S4, S6, S8, S10, S12 wells have no color observation, SKR4 S2 well is highly color observation due to the biofilm formation and the inhibitors added system have significantly reduced biofilm formation. The results of 570 nm in a UV-Visible spectrophotometer shows S3-0.093; S5-0.321; S7-0.469; S9-0.684; S11-0.952. The biofilm inhibition efficiency was ordered by MEAP > MERM > MEAM > MEPP > MEST as shown in Table 3. The biofilm assay's major striking feature S2 is that the bacterium *P. stutzeri* developed deep biofilm layers due to an excess of EPS production by SKR4 and it shows that *P. stutzeri* has the ability to form high biofilm layers on the surfaces (Ding et al., 2019; Wilson et al., 2017).

### 3.8. Weightloss method (WL)

The weight loss measurement examined corrosion rates and calculated the percentage of inhibition efficiency of 12 samples in the absence and presence of 25 ppm concentration of MEAP, MERM, MEAM, MEPP, MEST inhibitors against SKR4 on the MS 1010 with CTW. The weight loss results are given in Table 4 and it reveals that the maximum inhibition efficiency of 25 ppm concentration of inhibitors is MEAP 75 %, MERM, MEAM, MEPP, MEST are 71, 69, 66, 63 % respectively. The massive pitting corrosion was recorded in the S2, because of the presence of bacterial culture. Compared to the S2, inhibitors added systems of S3, S5, S7, S9, S11 recorded low corrosion rates was observed which inhibits corrosion by developing a protective barrier on the metal surface and S1, S4, S6, S8, S10, S12 only the inhibitor systems are mild corrosion was noted due to the presence of some inorganic compounds of the CTW. The high solubility of corrosion products induces the metal to lose its stability, which causes it to be dissolved by a solution. The weight loss of specimens linearly decreases in the corrosion rate with the addition of inhibitors (Shalabi et al., 2014).

### 3.9. Fourier transform infrared spectrophotometers (FT-IR) analysis

Functional groups of the biocorrosion products were identified using FTIR spectra and the presence and absence of inhibitors

**Table 3** Different Green Inhibitors in Variable Activities.

Inhibitors	Antibacterial activity (mm)	Minimal inhibition concentration ( $\mu\text{g}/\text{mL}$ )	Total viable count (CFU/mL)	Biofilm inhibition assay (OD)
MEAP	26	$18.18 \pm 1$	$1.0 \times 10^2$	0.093
MERM	19	$26.47 \pm 1$	$1.8 \times 10^3$	0.321
MEAM	15	$31.25 \pm 1$	$2.5 \times 10^3$	0.469
MEPP	11	$42.51 \pm 1$	$3.1 \times 10^3$	0.684
MEST	8	$65.13 \pm 1$	$3.9 \times 10^3$	0.957

**Table 4** Weight Loss Measurement for Biocorrosion Systems.

System	Weight Loss (mg)	Corrosion Rate (mm/y)	Inhibition Efficiency (%)
S1 - (Control - 500 mL flask with 400 mL of autoclaved CTW with 1 % NB medium)	29.35 ± 1	0.8009	–
S2 - (S1 + 100 µL + SKR4 culture)	326.76 ± 1	1.9999	–
S3 - (S2 + 25 ppm of MEAP)	119.59 ± 1	0.4988	75
S4 - (S1 + 25 ppm of MEAP)	15.78 ± 1	0.2669	58
S5 - (S2 + 25 ppm of MERM)	128.59 ± 1	0.3597	71
S6 - (S1 + 25 ppm of MERM)	19.83 ± 1	0.0445	57
S7 - (S2 + 25 ppm of MEAM)	135.73 ± 1	0.3921	69
S8 - (S1 + 25 ppm of MEAM)	23.09 ± 1	0.0467	55
S9 - (S2 + 25 ppm of MEPP)	145.51 ± 1	0.5739	66
S10 - (S1 + 25 ppm of MEPP)	27.66 ± 1	0.0473	54
S11 - (S2 + 25 ppm of MEST)	158.82 ± 1	0.6158	63
S12 - (S1 + 25 ppm of MEST)	31.74 ± 1	0.0494	52

**Table 5** FTIR Analysis for Biocorrosion Systems.

Peak Values (cm <sup>-1</sup> )	Bond	Intensity	Functional groups
839.61	O—H broad	weak-medium	Acids
3280.30	=C—H stretch (Alkenes)	weak, broad	Alkyl compounds
1630.55	N—H bend	medium-strong	Amides
1475.57	C—H bend	strong	Alkanes and Alkyls
1350.89	N—O <i>sym.</i> & <i>asym.</i> stretch C=C-NO <sub>2</sub> or Ar-NO <sub>2</sub>	strong	Nitro compounds
1152.46	C—O—C stretch	strong	Ethers
1107.49	C—O stretch	medium-strong	Alcohols
1022.28	C—O stretch	medium-strong	Phenols
875.10	C—H bend	strong	Alkenes
740.14	C-Cl (Chlorine)	strong	Halides
715.42	C—H bend (Alkanes)	medium	Alkyl compounds
703.03	≡C—H bend	strong, broad	Alkynes
580.24	C-I	strong	Halides
483.13	C-I stretch	strong	Alkyl halides

on the metal surface results are shown in Table 5 and Fig. 3. The corrosion products indicate that inhibitor's organic groups bind with the metal surface. The various bonds were identified in the dried corrosion samples. The OH stretch vibrations of the inhibitors have broadband in the range of 3839 cm<sup>-1</sup>. The weak intensity band of heteroaromatic = C—H stretch (Alkenes) was seen at 3280 cm<sup>-1</sup> and the intermolecular hydrogen bonding had wide bands and the C=C stretch, C—O stretch and C—O—C stretch phenols. Bond stretching was observed on 1621 cm<sup>-1</sup>, 1152 cm<sup>-1</sup>, and 1022 cm<sup>-1</sup> respectively. In the medium, strong intensity band at 1107 cm<sup>-1</sup>, the iron oxide peak showed a strong peak at 483 cm<sup>-1</sup> C-I stretch Alkyl halides. In the comparison of S2 and S3; S5; S7; S9; S11 the functional group peaks are shifted in the inhibitor's metal surface absorption frequencies providing solid evidence that the inhibitor's phytochemical components bind with the metal surface. It has been found that natural products containing phenolic compounds have strong antibacterial and corrosion inhibitions properties. In green inhibitors, the presence of aromatic substances such as oxygen, nitrogen, sulphur and lone-paired,  $\pi$ -electrons were shown to have a coordinating affinity for metal. As a result, electrons from the phenolic

OH group create a thick layer for protection of the iron complex and unoccupied d-orbital irons are shared to link the inhibitor molecules to the MS surface (Odewunmi et al., 2020; Salih et al., 2021).

### 3.10. Scanning electron microscopy (SEM) analysis

The results of SEM micrographs are used to examine the MS 1010 surface morphologies of SKR4 with various inhibitors shown in Fig. 4 (S1, S2, S3, S5, S7, S9, S11). The close examination of S2 samples revealed that the specimen surface was severely scratched accompanied by an aggressive attack of pitting formation. The corrosion scale looks on the S3, S5, S7, S9, and S11 sample surfaces look to be over uneven, with corrosion products layered on top of a metal surface. The MS had a smooth surface with a few little notches in the presence of inhibitors (S4, S6, S8, S10, S12), indicating that it may prevent iron dissolving, lowering the corrosion rate and providing more excellent (protective layer) corrosion protection. The various organic cation and anions can dissociate in an aqueous solution, changes in inhibitory behaviour should be attributed and action of the molecular structure. It was confirmed on the

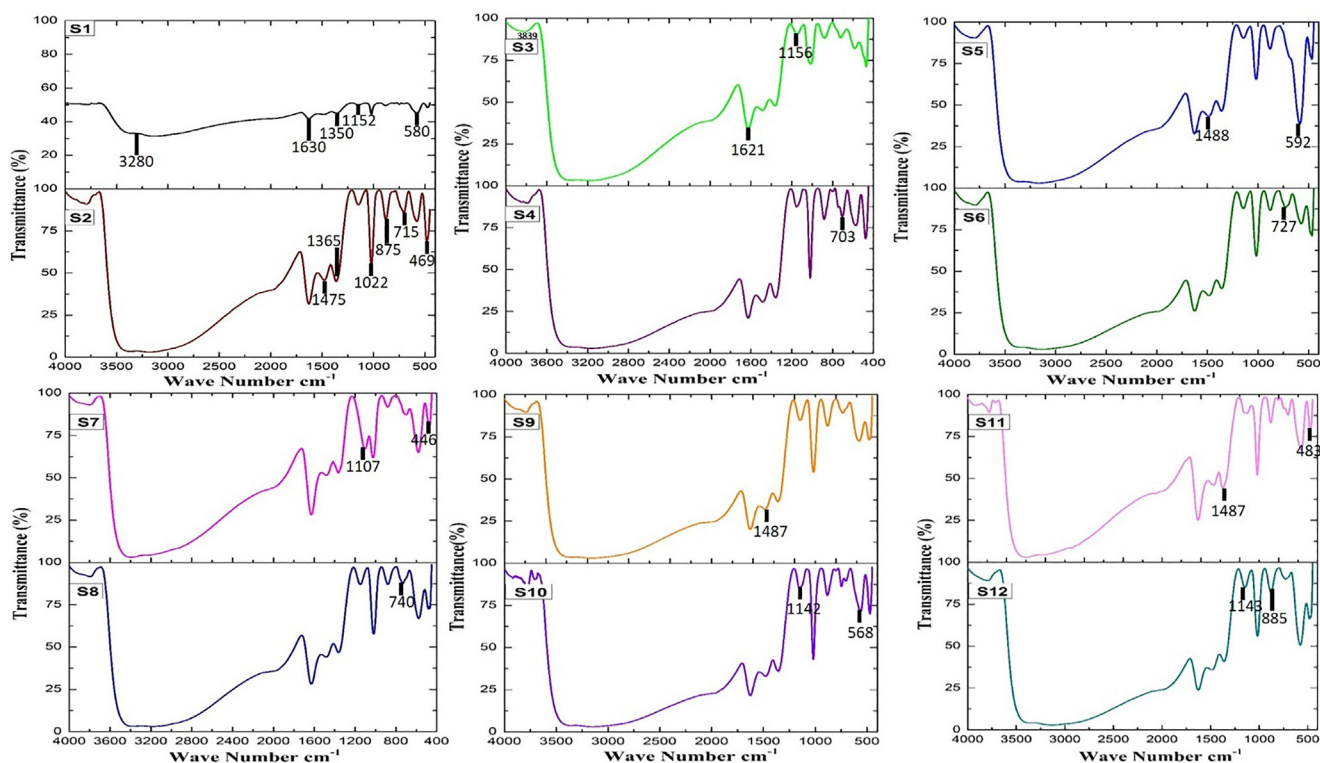


Fig. 3 FTIR Analysis for Biocorrosion Systems.

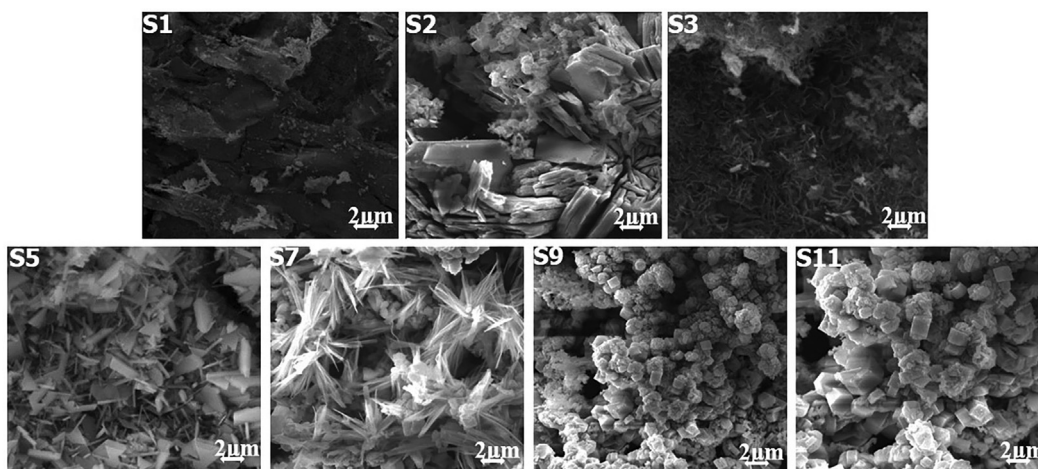


Fig. 4 SEM Analysis for Biocorrosion Systems.

metal surface, that the inhibitors create a great impact and prevent metal dissolution. The results suggest that the inhibitors added systems to slow down and restrict corrosion by being adsorbed on the sample surface (Rajasekar et al., 2005; Ramezanzadeh et al., 2014).

### 3.11. X-ray diffraction (XRD) studies

The XRD results showed the film formation on MS in the absence and presence of inhibitors in CTW. The metal scratched sample of systems (S1, S2, S3, S5, S7, S9, S11) and inhibitor adsorbed on an MS surface confirmed the protective film formation. The MS specimen had undergone corrosion,

leading to the formation of magnetite peaks due to the iron peaks that appeared in XRD spectra of MS surface SKR4 bacterial strain and the peaks are reduced containing an optimum concentration of the inhibitor extract as shown in Fig. 5 (Rajasekar et al., 2007). Carbon, nitrogen, oxygen and phytochemical compounds found in inhibitors may create a protective coating and reduce the iron peaks on metals.

### 3.12. Electrochemical studies

#### 3.12.1. Impedance spectroscopy

Nyquist plots of SKR4 bacterial solution on CTW in the absence of green inhibitors are shown in Table 6 and Fig. 6.

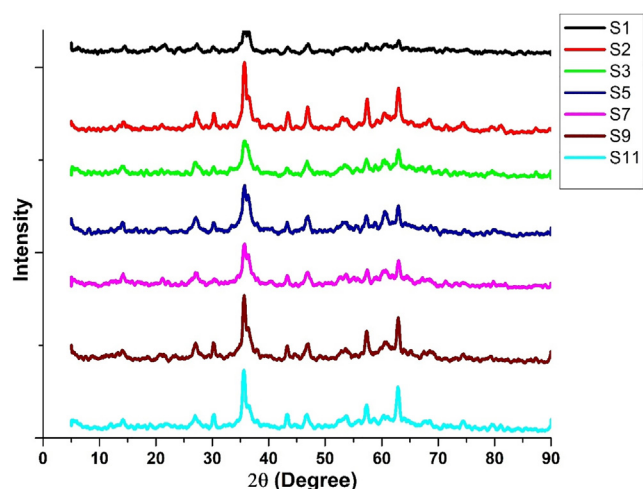


Fig. 5 XRD Analysis for Biocorrosion Systems.

Table 6 Electrochemical Impedance Parameters for Biocorrosion Systems.

System	$R_s$ ( $\Omega\text{cm}^2$ )	$R_{ct}$ ( $\Omega\text{cm}^2$ )
S1 - (Control - 500 mL flask with 400 mL of autoclaved CTW with 1 % NB medium)	-11.7	27
S2 - (S1 + 100 $\mu\text{L}$ + SKR4 culture)	-2.49	67
S3 - (S2 + 25 ppm of MEAP)	-4.99	54
S4 - (S1 + 25 ppm of MEAP)	-3.71	75
S5 - (S2 + 25 ppm of MERM)	-8.96	438
S6 - (S1 + 25 ppm of MERM)	-4.76	226
S7 - (S2 + 25 ppm of MEAM)	-2.37	469
S8 - (S1 + 25 ppm of MEAM)	-4.74	218
S9 - (S2 + 25 ppm of MEPP)	-4.69	725
S10 - (S1 + 25 ppm of MEPP)	-3.72	158
S11 - (S2 + 25 ppm of MEST)	-4.97	951
S12 - (S1 + 25 ppm of MEST)	-5.04	151

$R_s$  - Solution Resistance;  $R_{ct}$  - Charge transfer resistance

The Nyquist plots generated depressed semicircles typically related to the solid roughness, inhomogeneity and inhibitor adsorption on a metal surface. The impedance figure exposed the semicircle form of curves that confirmed corrosion reaction regulates through charge transfer. The impedance data is analyzed using the proper equivalent circuits based on geometries of Nyquist plots. In the absence and presence of inhibitors systems of equivalent circuit, as illustrated in Table 7 and Fig. 7 is employed to match the Nyquist plot in SKR4 bacterial solution with CTW. The working electrode surface roughness capacitance is calculated by one constant phase element (CPE), charge transfer resistance ( $R_{ct}$ ), polarization resistant ( $R_p$ ) and solution resistance ( $R_s$ ) then the double-layer capacitance (Cdl) to define the system's heterogeneity and surface layer resistance ( $R^2$ ). The CPE impedance is calculated using the following formula

$$Z(CPE) = Y_0^{-1}(j\omega)^{-n} \quad (2)$$

where  $Y_0$  denotes the magnitude of the CPE,  $j$  is the imaginary number,  $\omega$  is the angular frequency,  $n$  is the deviation param-

eter of the CPE:  $-1 \leq n \leq 1$ . If  $n = 1$ , CPE is capacitor; if  $n = 0$ , CPE is resistor; if  $n = -1$ , CPE is inductor; if  $n = 0.5$ , CPE is Warburg.  $Y_0$  has a dimension of  $s^n/\Omega$ , but the capacitance element (C) has  $s/\Omega$  or F and the differentiation,  $Y_0$  is commonly applied as though it were the capacitance of the corroding system (Socorro-Perdomo et al., 2021). The values of  $R_{ct}$  show that inhibitor compounds are bounded on the surface of MS specimens to create a protecting barrier, although controlled and slow down the corrosion process. The metal surface and inhibitors are attached through exchanging of electrons in between aromatic rings of hetero atoms and iron or  $\pi$  electron interaction. The adsorption took place on negatively charged metal surfaces with positively charged inhibitor molecules, forming a coordinating kind of bond between electrostatic interaction or charge transfer or sharing (Preethi Kumari et al., 2017). The  $R_{ct}$  values of experimental system S2 represent the presence of SKR4 absorbing a significant amount of current, indicating that the bacteria may have produced high corrosion on the metal, after the addition of inhibitors systems S3, S5, S7, S9, S11 shows low current consumption. The addition of green inhibitors has reduced current consumption as well as corrosion rates and the protective layers are formed to minimize microbial adhesion on a metal surface. The green inhibitors blocked EPS secretion through a binding mechanism of lone pair electrons (Narenkumar et al., 2018) and the inhibitor adsorption electron atoms are important to create protective barriers on the metal surface (Deyab, 2016).

### 3.12.2. Tafel polarization

Table 8 and Fig. 8 show Potentiodynamic Tafel polarization for MS 1010 coupons on CTW. The bacteria SKR4 was absence and presence of inhibitors on the specimen for anodic and cathodic polarization curves. The Tafel parameters are computed by corrosion potential ( $E_{corr}$ ), corrosion current density ( $i_{corr}$ ), cathodic slope ( $\beta_c$ ), corrosion rate (CR) and percentage of inhibition efficiency (% IE). The value of MS in the absence of inhibitors S2  $E_{corr}$  and  $i_{corr}$  value results in the potential to increase biofilm layer formation leading to pitting corrosion and high corrosion rate due to the SKR4 causing severe corrosion reaction and the presence of inhibitors controlling the corrosion current including the corrosion rate. At the optimal inhibitor concentration of 25 ppm, maximum efficiency in the range of S3, S5, S7, S9, S11 as 75, 71, 69, 66, 63 % respectively. As a consequence, lack of inhibitors exhibits a positive shift in the  $E_{corr}$  value, which indicates that the unbonded solution of inhibitors has the capacity to corrode by either an anodic or cathodic reaction. The presence of inhibitors shows an  $E_{corr}$  value at  $\pm 85$  mV indicating inhibitors act as a mixed type of inhibitors because it inhibits both hydrogen evolution reaction and metal hydrolysis. The atoms in chemical structures of inhibitors have lone pair electrons which helps to bind the unoccupied orbital of the metal ions, resulting from the covalent bond formation which reduces the corrosion rate and forms protective coatings. The impact of metal ion concentration on inhibitor sorption was investigated in this research. All the inhibitors have been identified to be efficient against biofilm formation, and act as good inhibitors and preventers (Kokalj and Peljhan, 2010). In this study confirmed that MEAP gives the best inhibition efficiency than the others MEAP > MERM > MEAM > MEPP > MEST.

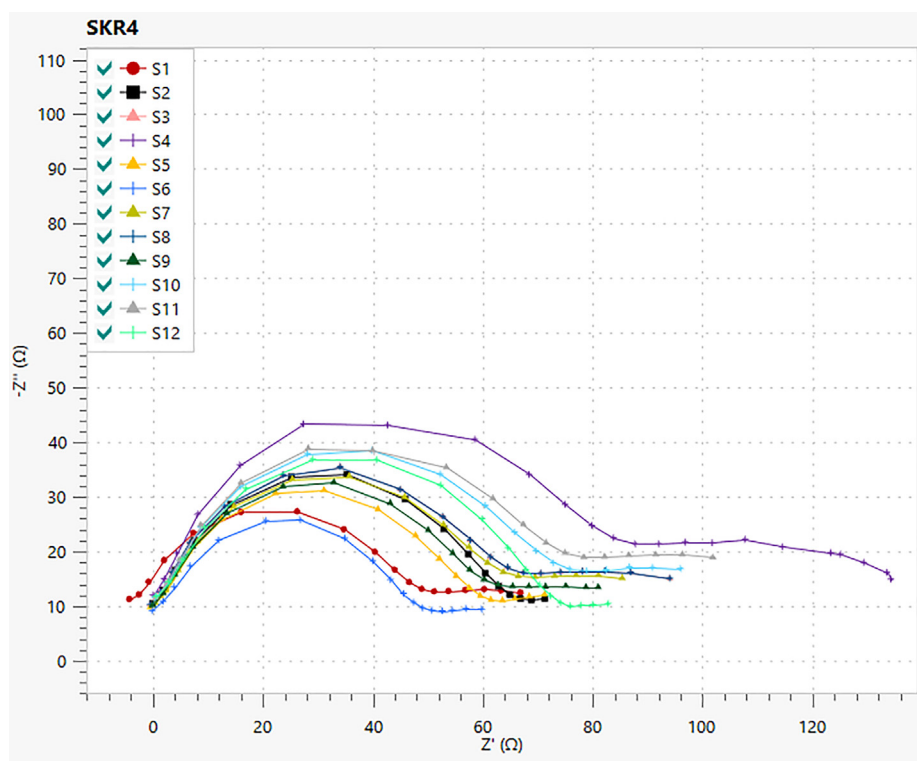


Fig. 6 Nyquist Plots for Biocorrosion Systems.

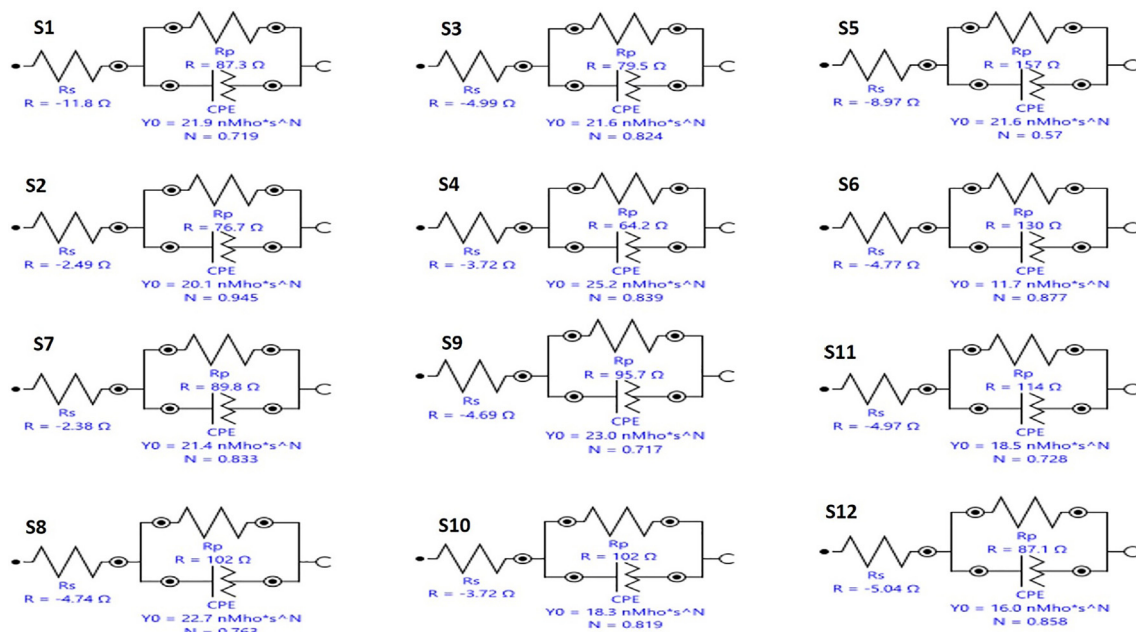
#### 4. Discussion

The organic or inorganic compounds are used as green inhibitors of metal surfaces to block the oxidation and reduction reaction in that inhibitors bind to the metal surface by their own adsorbing mechanism to create a protective layer. But still, inhibitors usage faced lots of environmental concerns of toxicity and hazards to living organisms, so it is difficult to use the inhibitors. In a number of research outcomes, green inhibitors are developing (plants, seaweeds and their parts) to inhibit the corrosion reaction in a natural way, they are all economically and eco-friendly (Khouzani et al., 2019; Okeniyi et al. 2014; Pino et al. 2001). The inhibitors are used to secure the metal surface through the formation of protecting film that primarily acts as a coating and provides protection throughout an organism's metabolic processes (Fouda et al., 2017a). The green inhibitors are used against microbial corrosion and it gives more effective results because of their organic compounds such as tannins, alkaloids, steroids, amino acids, flavonoids, etc. Microbes can cause 40 % of corrosion in the fields of oil, gas, water pipelines, cooling tower systems, and other things (Kokilaramani et al., 2021a). Using the inhibitors is necessary to prevent the MIC since green inhibitors have antibacterial properties. Biofilm-producing bacteria play an essential role in MIC that are difficult to remove from surfaces. The *Pseudomonas* species produce huge biofilm layers that have a wide range of different adhesions functions during initial attachment to a surface (Rossell6-Moral9 et al., 1994). There are three primary processes in the absorption of metal ions with an adsorbent that is the target metal migrates the solution to the adsorbent's surface, metal diffusion across the boundary layer and final one is the target metal's sorption to a particular adsorption site (Gupta et al., 2010; Kip and van Veen, 2015).

The previous studies reported (Fouda et al., 2017b; Pineda Hernández et al., 2021; Shitole et al., 2014) that mangrove leaves and seaweeds have a good inhibition efficiency on the various metals in various mediums. The phytochemical components of the inhibitors work synergistically to prevents development of microbes and the secretion of their metabolism, which cause passivity and excellent inhibition in the various test medium. The biofilm layers play a vital role in MIC, which was help to develop corrosion on the metal then surface analysis and electrochemical techniques are used to investigate the corrosion and protection mechanisms (Gunasekaran et al., 2004). The vacant d-orbital of a metal surface and  $\pi$ -electrons of aromatic rings in inhibitors interaction between donor-acceptor interactions as well as unshared pair electrons of N, S, O, and d-orbital electrons of the iron surface have interacted. It has revealed details about corrosion and protection, notably in the presence of adsorbed chemical/biochemical species and an organic coating. Green inhibitors work so well because they contain organic compounds with oxygen, sulphur, and nitrogen atoms in the molecule that act as an active center for the absorption process by forming protective barriers with the aid of strong interactions like orbital adsorption, chemisorption, and electrostatic adsorption on a metal surface to minimize the corrosion attack. (Odusote and Ajayi, 2013). The behavior of MS in CTW-containing microbes was investigated in the current study and inhibitory action (Shah et al., 2011). The fact that corrosion rate lowers as the inhibitor concentration increases suggest that the inhibitor concentration is a factor in the corrosion rate. According to this study MEAP, MERM, MEAM, MEPP, MEST are used as corrosion inhibitors in the industrial circulating CTW systems with high environmental protection and safety standards. The novelty of this study was to use of green organic compounds found in leaves

**Table 7** Equivalent Circuits for Biocorrosion System.

<b>S1</b>	Element	Parameter	Value	<b>S3</b>	Element	Parameter	Value	<b>S5</b>	Element	Parameter	Value
	Rs	R	-11.758		Rs	R	-4.9927		Rs	R	-8.9657
	Rp	R	87.258		Rp	R	79.54		Rp	R	157.14
	CPE	Y0	2.1907E-08		CPE	Y0	2.1569E-08		CPE	Y0	2.1557E-08
		N	0.71945			N	0.82436			N	0.57033
<b>S2</b>	Element	Parameter	Value	<b>S4</b>	Element	Parameter	Value	<b>S6</b>	Element	Parameter	Value
	Rs	R	-2.4918		Rs	R	-3.7155		Rs	R	-4.7697
	Rp	R	76.697		Rp	R	64.21		Rp	R	130.01
	CPE	Y0	2.0118E-08		CPE	Y0	2.5173E-08		CPE	Y0	1.1686E-08
		N	0.94526			N	0.83884			N	0.87723
<b>S7</b>	Element	Parameter	Value	<b>S9</b>	Element	Parameter	Value	<b>S11</b>	Element	Parameter	Value
	Rs	R	-2.375		Rs	R	-4.6917		Rs	R	-4.9744
	Rp	R	89.821		Rp	R	95.658		Rp	R	114.17
	CPE	Y0	2.1386E-08		CPE	Y0	2.302E-08		CPE	Y0	1.8512E-08
		N	0.83322			N	0.71696			N	0.72819
<b>S8</b>	Element	Parameter	Value	<b>S10</b>	Element	Parameter	Value	<b>S12</b>	Element	Parameter	Value
	Rs	R	-4.7404		Rs	R	-3.7249		Rs	R	-5.0406
	Rp	R	101.65		Rp	R	101.94		Rp	R	87.105
	CPE	Y0	2.268E-08		CPE	Y0	1.8283E-08		CPE	Y0	1.6023E-08
		N	0.76332			N	0.81915			N	0.8584

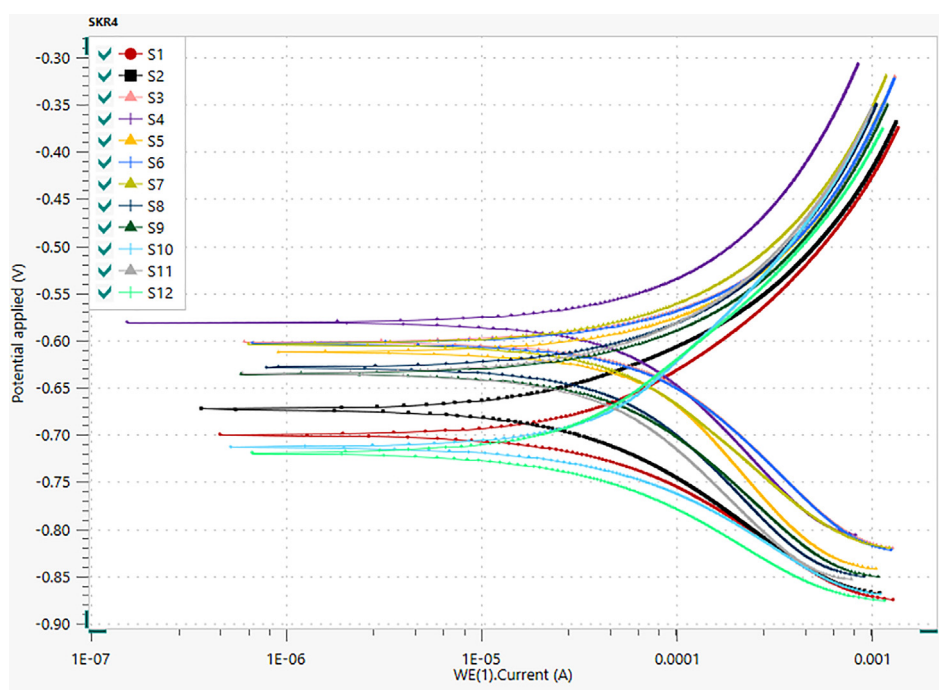


**Fig. 7** Equivalent Circuit for Biocorrosion Systems.

**Table 8** Tafel Potentiodynamic Polarization Parameters for Biocorrosion Systems.

System	$E_{corr}$ (V)	$i_{corr}$ (A $cm^{-2}$ )	$\beta_a$ (V/dec)	$\beta_c$ (V/dec)	$R_p$ ( $K\Omega cm^2$ )
S1 - (Control - 500 mL flask with 400 mL of autoclaved CTW with 1 % NB medium)	-0.699	14.9251	0.1758	-0.1420	696.49
S2 - (S1 + 100 $\mu$ L + SKR4 culture)	-0.972	83.5092	0.1286	-0.1477	851.14
S3 - (S2 + 25 ppm of MEAP)	-0.610	23.7639	0.2069	-0.4892	450.01
S4 - (S1 + 25 ppm of MEAP)	-0.602	2.1451	0.1887	-0.4373	394.52
S5 - (S2 + 25 ppm of MERM)	-0.613	27.8437	0.1475	-0.2130	482.60
S6 - (S1 + 25 ppm of MERM)	-0.580	3.3973	0.2329	-0.4817	550.97
S7 - (S2 + 25 ppm of MEAM)	-0.628	29.1091	0.2116	-0.3526	564.26
S8 - (S1 + 25 ppm of MEAM)	-0.603	5.4456	0.1703	-0.2652	533.44
S9 - (S2 + 25 ppm of MEPP)	-0.635	31.6555	0.1788	-0.2361	577.45
S10 - (S1 + 25 ppm of MEPP)	-0.512	7.3907	0.4380	-0.1539	669.23
S11 - (S2 + 25 ppm of MEST)	-0.634	35.1785	0.1833	-0.2866	676.38
S12 - (S1 + 25 ppm of MEST)	-0.618	9.53189	0.1969	-0.1208	920.87

$E_{corr}$  - Corrosion Potential;  $i_{corr}$  - Corrosion Current Density;  $\beta_a$  - Anode Beta coefficient;  $\beta_c$  - Cathode Beta coefficient;  $R_p$  - Polarization Resistance; mV/dec - Millivolt/Decade

**Fig. 8** Tafel Polarization Plots for Biocorrosion Systems.

and seaweeds which significantly contributed to the reducing biocorrosion inhibitor for mild steel in CTW by approximately 70 % under these experimental circumstances. The different test conditions from various aspects can help raise the percentage of corrosion resistance. In most cases, the findings are superior to those found in the literature because different plant extracts have varied corrosion inhibiting capabilities.

## 5. Conclusion

The present study shows that MEAP was a superior inhibitor of corrosion in MS 1010 on the CTW with SKR4 bacteria when compared to MERM, MEAM, MEPP, and MEST. GCMS was used to study green inhibitor compounds, which demonstrate that have antimicro-

bial activities and control the biofilm film formation by inhibiting microbial metabolic activities. The iron complex forms a thin coating on the MS surface, indicating a molecular structure of the inhibitor compounds binds the metal ions, as seen by FTIR spectra of biocorrosion samples. The inhibitor absorbs existence of d-orbitals electrons on iron surface between the phenolic group of unoccupied vacant of inhibitor phytochemical compounds and MS surface. The polarization study supported that the MEAP treated systems had lower corrosion currents than other systems. The electrochemical studies of EIS and polarization are favorable to this range MEAP > MERM > MEAM > MEPP > MEST and act as a mixed type of inhibitor. Future studies will examine which bioactive compounds in green extracts have the potential to reduce corrosion. The bioactive components in the extract will be separated and used individually in corrosion testing. More investigation may be done to see

whether or not all bioactive chemicals interact to form inhibitors and whether these chemicals can prevent corrosion on their own or in conjunction with other substances.

## 6. Ethics approval

This article does not contain any studies with human participants or animals performed by any of the authors.

## 7. Consent for publication

All authors agreed to publish this version of the article.

## 8. Availability of data and materials

The datasets used and analyzed during the current study are available from the corresponding author on reasonable request.

## Declaration of Competing Interest

The authors declare that they have no known competing financial interests or personal relationships that could have appeared to influence the work reported in this paper.

## Acknowledgment

The authors extend their appreciation to the Deputyship for Research & Innovation, Ministry of Education in Saudi Arabia for funding this research work through the project no. (IFKSURG-2-527).

## Appendix A. Supplementary material

Supplementary data to this article can be found online at <https://doi.org/10.1016/j.arabjc.2022.104513>.

## References

- Ahmed, S.-A.-R., Makki, H.F., 2019. Corrosion rate optimization of mild-steel under different cooling tower working parameters using Taguchi design. *J. Eng.* 26, 174–185. <https://doi.org/10.31026/j.eng.2020.01.13>.
- Al Otaibi, N., Hammud, H.H., 2021. Corrosion inhibition using harmal leaf extract as an eco-friendly corrosion inhibitor. *Molecules* 26. <https://doi.org/10.3390/molecules26227024>.
- Ashraf Ismail, N., Moussa, A.M., Kahraman, R., Shakoor, R.A., 2022. Study on the corrosion behavior of polymeric nanocomposite coatings containing halloysite nanotubes loaded with multicomponent inhibitor. *Arab. J. Chem.* 15. <https://doi.org/10.1016/j.arabjc.2022.104107> 104107.
- Cherrad, S., Alrashdi, A.A., Lee, H.S., el aoufir, Y., Lgaz, H., Satrani, B., Ghanmi, M., Aouane, E.M., Chaouch, A., 2022. Cupressus arizonica fruit essential oil: A novel green inhibitor for acid corrosion of carbon steel: Cupressus arizonica fruit essential oil. *Arabian Journal of Chemistry* 15. <https://doi.org/10.1016/j.arabjc.2022.103849>
- Deyab, M.A., 2016. Inhibition activity of Seaweed extract for mild carbon steel corrosion in saline formation water. *Desalination* 384, 60–67. <https://doi.org/10.1016/j.desal.2016.02.001>.
- Ding, X.S., Zhao, B., An, Q., Tian, M., Guo, J.S., 2019. Role of extracellular polymeric substances in biofilm formation by *Pseudomonas stutzeri* strain XL-2. *Appl. Microbiol. Biotechnol.* 103, 9169–9180. <https://doi.org/10.1007/s00253-019-10188-4>.
- Feijoo-Siota, L., Rosa-Dos-Santos, F., de Miguel, T., Villa, T.G., 2008. Biodegradation of naphthalene by *Pseudomonas stutzeri* in marine environments: testing cells entrapment in calcium alginate for use in water detoxification. *Bioremediat. J.* 12, 185–192. <https://doi.org/10.1080/10889860802477168>.
- Fouda, A.S., Fayed, T., Elmorsi, M.A., Elsayed, M., 2017b. Distyryl derivatives as corrosion inhibitors for carbon steel in acid cleaning process in cooling towers. *Journal of Bio-and Tribo-Corrosion* 3 (3), 1–18. <https://doi.org/10.1007/s40735-017-0093-0>.
- Fouda, A.S., Rashwan, S.M., Kamel, M.M., Arman, N.M., 2017a. Adsorption and inhibition behavior of *Avicennia marina* for Zn metal in hydrochloric acid solution. *Int. J. Electrochem. Sci.* 12, 11789–11804. <https://doi.org/10.20964/2017.12.95>.
- K. M. O. Goni, L., A. J. Mazumder, M., 2019. Green Corrosion Inhibitors, in: *Corrosion Inhibitors*. IntechOpen. <https://doi.org/10.5772/intechopen.81376>
- unasekaran, G., Chongdar, S., Gaonkar, S.N., Kumar, P., 2004. Influence of bacteria on film formation inhibiting corrosion. *Corros Sci* 46, 1953–1967. <https://doi.org/10.1016/j.corsci.2003.10.023>
- Gupta, S., Prakash, R., Prakash, N.T., Pearce, C., Patrick, R., Hery, M., Lloyd, J., 2010. Selenium mobilization by *Pseudomonas aeruginosa* (SNT-SG1) isolated from seleniferous soils from India. *Geomicrobiol. J.* 27, 35–42. <https://doi.org/10.1080/01490450903232173>.
- Huang, L., Yang, K.P., Zhao, Q., Li, H.J., Wang, J.Y., Wu, Y.C., 2022. Corrosion resistance and antibacterial activity of procyanidin B2 as a novel environment-friendly inhibitor for Q235 steel in 1 M HCl solution. *Bioelectrochemistry* 143. <https://doi.org/10.1016/j.bioelechem.2021.107969>.
- Ismail, N., Mujad, S.M., Fakhratul, M., Zulkifli, R., Izionworu, V.O., Ghazali, M.J., Norsani, W.M., Nik, W., 2022. Cite this paper. *Vietnam J. Chem* 2022, 60. <https://doi.org/10.1002/vjch.202200001>
- Kakooei, S., Ismail, C., Ariwahjoedi, B., 2012. Mechanisms of microbiologically influenced corrosion: a review. *World Appl. Sci. J.* 17, 524–531.
- Kamil, Z., Al-Hassani, K., n.d. Isolation and Identification of *Pseudomonas stutzeri* Isolated from Intrauterine Devices. *University Journal for Biology* 8, 2016.
- Karunakaran, E., Biggs, C.A., 2011. Mechanisms of *Bacillus cereus* biofilm formation: an investigation of the physicochemical characteristics of cell surfaces and extracellular proteins. *Appl. Microbiol. Biotechnol.* 89, 1161–1175. <https://doi.org/10.1007/s00253-010-2919-2>.
- Khattab, R.A., Gaballa, A., Zakaria, S.M., Allah, A., Ali, E.-S., Sultan Sallam, I., Temraz, T., 2012. Phytochemical Analysis of *Avicennia marina* and *Rhizophora mucronata* by GC-MS, CATRINA.
- Khouzani, M.K., Bahrami, A., Hosseini-Abari, A., Khandouzi, M., Taheri, P., 2019. Microbiologically influenced corrosion of a pipeline in a petrochemical plant. *Metals (Basel)* 9. <https://doi.org/10.3390/met9040459>.
- Kip, N., van Veen, J.A., 2015. The dual role of microbes in corrosion. *ISME J.* <https://doi.org/10.1038/ismej.2014.169>.
- Kokalj, A., Peljhan, S., 2010. Density functional theory study of ATA, BTAH, and BTAOH as copper corrosion inhibitors: Adsorption onto Cu(111) from gas phase. *Langmuir* 26, 14582–14593. <https://doi.org/10.1021/la1019789>.
- Kokilaramani, S., AlSalhi, M.S., Devanesan, S., Narenkumar, J., Rajasekar, A., Govarthanam, M., 2020. *Bacillus megaterium*-induced biocorrosion on mild steel and the effect of *Artemisia pallens* methanolic extract as a natural corrosion inhibitor. *Arch. Microbiol.* 202, 2311–2321. <https://doi.org/10.1007/s00203-020-01951-7>.
- Kokilaramani, S., Al-Ansari, M.M., Rajasekar, A., Al-Khattaf, F.S., Hussain, A.M.R., Govarthanam, M., 2021a. Microbial influenced corrosion of processing industry by re-circulating waste water and

- its control measures - a review. *Chemosphere*. <https://doi.org/10.1016/j.chemosphere.2020.129075>.
- Kokilaramani, S., Rajasekar, A., AlSalhi, M.S., Devanesan, S., 2021b. Characterization of methanolic extract of seaweeds as environmentally benign corrosion inhibitors for mild steel corrosion in sodium chloride environment. *J. Mol. Liq.* 340. <https://doi.org/10.1016/j.molliq.2021.117011>.
- Kokilaramani, S., Narenkumar, J., AlSalhi, M.S., Devanesan, S., Obulisamy, P.K., Balagurunathan, R., Rajasekar, A., 2022. Evaluation of crude methanolic mangrove leaves extract for antibiofilm efficacy against biofilm-forming bacteria on a cooling tower wastewater system. *Arab. J. Chem.* 15. <https://doi.org/10.1016/j.arabjc.2022.103948> 103948.
- Kuraimid, Z.K., Majeed, H.M., Jebur, H.Q., Ahmed, T.S., Jaber, O. S., 2021. Synthesis of new corrosion inhibitors with high efficiency in aqueous and oil phase for low carbon steel for missan oil field equipment. *Eurasian Chem. Commun.* 3, 860–871. <https://doi.org/10.22034/ecc.2021.302887.1233>.
- Lalucat, J., Bennasar, A., Bosch, R., García-Valdés, E., Palleroni, N. J., 2006. Biology of *Pseudomonas stutzeri*. *Microbiol. Mol. Biol. Rev.* 70, 510–547. <https://doi.org/10.1128/mmlbr.00047-05>.
- Maleki, B., Davoodi, A., Azghandi, M.V., Baghayeri, M., Akbarzadeh, E., Veisi, H., Ashrafi, S.S., Raei, M., 2016. Facile synthesis and investigation of 1,8-dioxooctahydroxanthene derivatives as corrosion inhibitors for mild steel in hydrochloric acid solution. *New J. Chem.* 40, 1278–1286. <https://doi.org/10.1039/c5nj02707a>.
- Mobin, M., Ahmad, I., Basik, M., Murmu, M., Banerjee, P., 2020. Experimental and theoretical assessment of almond gum as an economically and environmentally viable corrosion inhibitor for mild steel in 1 M HCl. *Sustain. Chem. Pharm.* 18. <https://doi.org/10.1016/j.scp.2020.100337>.
- Muthukrishnan, P., Jeyaprabha, B., Prakash, P., 2017. Adsorption and corrosion inhibiting behavior of *Lannea coromandelica* leaf extract on mild steel corrosion. *Arab. J. Chem.* 10, S2343–S2354. <https://doi.org/10.1016/j.arabjc.2013.08.011>.
- Narenkumar, J., Parthipan, P., Madhavan, J., Murugan, K., Marpu, S.B., Suresh, A.K., Rajasekar, A., 2018. Bioengineered silver nanoparticles as potent anti-corrosive inhibitor for mild steel in cooling towers. *Environ. Sci. Pollut. Res.* 25, 5412–5420. <https://doi.org/10.1007/s11356-017-0768-6>.
- Narenkumar, J., Devanesan, S., AlSalhi, M.S., Kokilaramani, S., Ting, Y.P., Rahman, P.K.S.M., Rajasekar, A., 2021. Biofilm formation on copper and its control by inhibitor/biocide in cooling water environment. *Saudi J. Biol. Sci.* 28, 7588–7594. <https://doi.org/10.1016/j.sjbs.2021.10.012>.
- Narenkumar, J., Parthipan, P., Usha Raja Nanthini, A., Benelli, G., Murugan, K., Rajasekar, A., 2017a. Ginger extract as green biocide to control microbial corrosion of mild steel. *3 Biotech* 7. <https://doi.org/10.1007/s13205-017-0783-9>.
- Obot, I.B., Obi-Egbedi, N.O., Umoren, S.A., 2009. Antifungal drugs as corrosion inhibitors for aluminium in 0.1 M HCl. *Corros. Sci.* 51, 1868–1875. <https://doi.org/10.1016/j.corsci.2009.05.017>.
- Odeunmi, N.A., Solomon, M.M., Umoren, S.A., Ali, S.A., 2020. Comparative studies of the corrosion inhibition efficacy of a dicationic monomer and its polymer against API X60 steel corrosion in simulated acidizing fluid under static and hydrodynamic conditions. *ACS Omega* 5, 27057–27071. <https://doi.org/10.1021/acsomega.0c02345>.
- Odusote, J.K., Ajayi, O.M., 2013. Corrosion inhibition of mild steel in acidic medium by *Jathropa Curcas* leaves extract. *J. Electrochem. Sci. Technol.* 4, 81–87. <https://doi.org/10.5229/jecst.2013.4.2.81>.
- Oguzie, Emeka Emmanuel, Iroha, N.B., Oguzie, E E, Onuoha, G.N., Onuchukwu, A.I., 2005. INHIBITION OF MILD STEEL CORROSION IN ACIDIC SOLUTION BY DERIVATIVES OF DIPHENYL GLYOXAL.
- Okeniyi, J.O., Ikotun, J.O., Akinlabi, E.T., Okeniyi, E.T., 2019. Anticorrosion Behaviour of *Rhizophora mangle* L. Bark-Extract on Concrete Steel-Rebar in Saline/Marine Simulating-Environment. *Scientific World Journal* 2019. <https://doi.org/10.1155/2019/6894714>
- Okeniyi, J.O., Loto, C.A., Popoola, A.P.I., 2014. *Rhizophora mangle* L. effects on steel-reinforced concrete in 0.5 M H<sub>2</sub>SO<sub>4</sub>: Implications for corrosion-degradation of wind-energy structures in industrial environments. In: *Energy Procedia*. Elsevier Ltd, pp. 429–436. <https://doi.org/10.1016/j.egypro.2014.06.052>.
- Pineda Hernández, D.A., Restrepo Parra, E., Arango Arango, P.J., Segura Giraldo, B., Acosta Medina, C.D., 2021. Article innovative method for coating of natural corrosion inhibitor based on *artemisia vulgaris*. *Materials* 14. <https://doi.org/10.3390/ma14092234>.
- Pino, J.A., Marbot, R., Agüero, J., Sánchez, L.M., 2001. Volatile components of red mangrove bark (*rhizophora mangle* l.) from Cuba. *J. Essent. Oil Res.* 13, 88–89. <https://doi.org/10.1080/10412905.2001.9699622>.
- Pipattanachit, S., Qin, J., Rokaya, D., Thanyasrisung, P., Srimaneep-ong, V., 2021. Biofilm inhibition and bactericidal activity of NiTi alloy coated with graphene oxide/silver nanoparticles via electrophoretic deposition. *Sci. Rep.* 11. <https://doi.org/10.1038/s41598-021-92340-7>.
- Popova, A., Sokolova, E., Raicheva, S., Christov, M., n.d. AC and DC study of the temperature effect on mild steel corrosion in acid media in the presence of benzimidazole derivatives.
- Popova, A., Vasilev, A., Deligeorgiev, T., 2018. Evaluation of the electrochemical impedance measurement of mild steel corrosion in an acidic medium, in the presence of quaternary ammonium bromides. *Port. Electrochim. Acta* 36, 423–435. <https://doi.org/10.4152/pea.201806423>.
- Preethi Kumari, P., Shetty, P., Rao, S.A., 2017. Electrochemical measurements for the corrosion inhibition of mild steel in 1 M hydrochloric acid by using an aromatic hydrazide derivative. *Arab. J. Chem.* 10, 653–663. <https://doi.org/10.1016/j.arabjc.2014.09.005>.
- Quraishi, M.A., Chauhan, D.S., Ansari, F.A., 2021. Development of environmentally benign corrosion inhibitors for organic acid environments for oil-gas industry. *J. Mol. Liq.* <https://doi.org/10.1016/j.molliq.2021.115514>.
- Rajasekar, A., Maruthamuthu, S., Muthukumar, N., Mohanan, S., Subramanian, P., Palaniswamy, N., 2005. Bacterial degradation of naphtha and its influence on corrosion. *Corros. Sci.* 47, 257–271. <https://doi.org/10.1016/j.corsci.2004.05.016>.
- Rajasekar, A., Ganesh Babu, T., Karutha Pandian, S., Maruthamuthu, S., Palaniswamy, N., Rajendran, A., 2007. Biodegradation and corrosion behavior of manganese oxidizer *Bacillus cereus* ACE4 in diesel transporting pipeline. *Corros. Sci.* 49, 2694–2710. <https://doi.org/10.1016/j.corsci.2006.12.004>.
- Rajasekar, A., Maruthamuthu, S., Ting, Y.P., 2008. Electrochemical behavior of *Serratia marcescens* ACE2 on carbon steel API 5L–X60 in organic/aqueous phase. *Ind. Eng. Chem. Res.* 47, 6925–6932. <https://doi.org/10.1021/ie8005935>.
- Rajasekar, A., Anandkumar, B., Maruthamuthu, S., Ting, Y.P., Rahman, P.K.S.M., 2010. Characterization of corrosive bacterial consortia isolated from petroleum-product-transporting pipelines. *Appl. Microbiol. Biotechnol.* 85, 1175–1188. <https://doi.org/10.1007/s00253-009-2289-9>.
- Ramezanzadeh, B., Mehdipour, M., Arman, S.Y., Professor, A., 2014. Application of Electrochemical Noise to Investigate Corrosion Inhibition Properties of Some Azole Compounds on Aluminum in 0.25 M HCl.
- Rossell6-Moral9, R.A., Lalucat, J., Dott2, W., Kampfer2, P., 1994. Biochemical and chemotaxonomic characterization of *Pseudomonas stutzeri* genomovars, *Journal of Applied Bacteriology*.
- Salih, A.R., Al-Messri, A.K., Al-Messri, Z.A.K., 2021. Synthesis of pyranopyrazole and pyranopyrimidine derivatives using magnesium oxide nanoparticles and evaluation as corrosion inhibitors for lubricants. *Eurasian Chem. Commun.* 3, 533–541. <https://doi.org/10.22034/ecc.2021.291144.1189>.

- Shah, A.M., Rahim, A.A., Yahya, S., Raja, P.B., Hamid, S.A., 2011. Acid corrosion inhibition of copper by mangrove tannin. *Pigm. Resin Technol.* 40, 118–122. <https://doi.org/10.1108/03699421111113783>.
- Shalabi, K., Shalabi, K., Abdallah, Y., Hassan, H.M., Fouda, A., 2014. Adsorption and Corrosion Inhibition of Atropa Belladonna Extract on Carbon Steel in 1 M HCl Solution. *Int. J. Electrochem. Sci.*
- Shitole, S.S., Balange, A.K., Gangan, S.S., 2014. Use of Seaweed (*Sargassum tenerrimum*) extract as gel enhancer for lesser sardine (*Sardinella brachiosoma*) surimi. *Int. Aquat. Res.* 6, 1–11. <https://doi.org/10.1007/s40071-014-0055-9>.
- Socorro-Perdomo, P.P., Florido-Suárez, N.R., Voiculescu, I., Mirza-Rosca, J.C., 2021. Comparative eis study of alxcoerfeni alloys in ringer's solution for medical instruments. *Metals (Basel)* 11. <https://doi.org/10.3390/met11060928>.
- Suharso, Reno, T., Endaryanto, T., Buhani, 2017. Modification of Gambier extracts as green inhibitor of calcium carbonate (CaCO<sub>3</sub>) scale formation. *Journal of Water Process Engineering* 18, 1–6. <https://doi.org/10.1016/j.jwpe.2017.05.004>
- Thakur, A., Kumar, A., 2021. Sustainable inhibitors for corrosion mitigation in aggressive corrosive media: a comprehensive study. *J. Bio Tribocorros.* <https://doi.org/10.1007/s40735-021-00501-y>.
- Verma, C., Quraishi, M.A., Ebenso, E.E., Hussain, C.M., 2021. Recent advancements in corrosion inhibitor systems through carbon allotropes: past, present, and future. *Nano Select* 2, 2237–2255. <https://doi.org/10.1002/nano.202100039>.
- Wagner, T. v., Parsons, J.R., Rijnaarts, H.H.M., de Voogt, P., Langenhoff, A.A.M., 2018. A review on the removal of conditioning chemicals from cooling tower water in constructed wetlands. *Crit Rev Environ Sci Technol* 48, 1094–1125. <https://doi.org/10.1080/10643389.2018.1512289>
- Wang, S., Sun, J., Shan, B., Fan, W., Ding, R., Yang, J., Zhao, X., 2022. Performance of dodecyl dimethyl benzyl ammonium chloride as bactericide and corrosion inhibitor for 7B04 aluminum alloy in an aircraft fuel system. *Arab. J. Chem.* 15. <https://doi.org/10.1016/j.arabjc.2022.103926>.
- Wang, D., Xu, A., Elmerich, C., Ma, L.Z., 2017. Biofilm formation enables free-living nitrogen-fixing rhizobacteria to fix nitrogen under aerobic conditions. *ISME J.* 11, 1602–1613. <https://doi.org/10.1038/ismej.2017.30>.
- Wilson, C., Valquier-Flynn, H., Sandoval, J., Okuom, M.O., 2017. Quantitative and Qualitative Assessment Methods for Biofilm Growth: A Mini-review Architecture of Biofilm Growth View project statistical mechanics of magnetic systems View project.
- Zaher, A., Aslam, R., Lee, H.S., Khafouri, A., Boufellous, M., Alrashdi, A.A., el aoufir, Y., Lgaz, H., Ouhssine, M., 2022. A combined computational & electrochemical exploration of the Ammi visnaga L. extract as a green corrosion inhibitor for carbon steel in HCl solution. *Arabian Journal of Chemistry* 15. <https://doi.org/10.1016/j.arabjc.2021.103573>
- Zakeri, A., Bahmani, E., Aghdam, A.S.R., 2022. Plant extracts as sustainable and green corrosion inhibitors for protection of ferrous metals in corrosive media: a mini review. *Corros. Commun.* <https://doi.org/10.1016/j.corcom.2022.03.002>.
- Zehra, S., Mobin, M., Aslam, R., 2022. Corrosion inhibitors: an introduction, in: *Environmentally Sustainable Corrosion Inhibitors*. Elsevier, pp. 47–67. <https://doi.org/10.1016/b978-0-323-85405-4.00022-7>
- Zhang, H., Liu, D., Zhao, L., Wang, J., Xie, S., Liu, S., Lin, P., Zhang, X., Chen, C., 2022. Review on corrosion and corrosion scale formation upon unlined cast iron pipes in drinking water distribution systems. *J. Environ. Sci.* <https://doi.org/10.1016/j.jes.2022.04.024>.